SEMICONDUCTORS AND DIELECTRICS

V.V. HALYAN,[1] A.H. KEVSHYN,[1] I.A. IVASHCHENKO,[2] T.K. YATSYNIUK,[1]
B.A. TATARYN,[3] M.A. SKORYK,[4] O.O. LEBED,[5] V.O. YUKHYMCHUK [6]

[1] Department of Experimental Physics, Information and Education Technologies,
  Lesya Ukrainka Volyn National University
  (13, Voli Ave., Lutsk 43000, Ukraine)
[2] Faculty of Chemical Engineering and Technology, Cracow University of Technology
  (Warszawska St. 24, 31-155 Cracow, Poland)
[3] Department of Chemistry and Technology, Lesya Ukrainka Volyn National University
  (13, Voli Ave., Lutsk 43000, Ukraine)
[4] G.V. Kurdyumov Institute for Metal Physics, Nat. Acad. of Sci. of Ukraine
  (Kyiv 03142, Ukraine)
[5] National University of Water and Environmental Engineering
  (11, Soborna Str. Rivne 33000, Ukraine)
[6] V. Lashkaryov Institute of Semiconductor Physics, Nat. Acad. of Sci.
  (45, Prosp. Nauky, Kyiv 03028, Ukraine)

NEAR- AND MID-INFRARED EMISSIONS FROM Ga_2S_3–GeS_2–Sb_2S_3: Er, Nd GLASSES

Glasses of 20 mol.% Ga_2S_3 – 60 mol.% GeS_2 – 20 mol.% Sb_2S_3: Er_2S_3 (1–4 mol.%); Nd_2S_3 (2 mol.%) composition were obtained by the quenching technique. The optical absorption spectra investigation established that maxima at 655, 755, 810, 885, 980, and 1540 nm are the main absorption bands. Upon excitation of PL by radiation with $\lambda = 805$ nm, bands with maxima at 1070, 1350, 1540, 1700, and 2490 nm appear in the spectrum, which corresponds to the transitions $^4F_{3/2} \rightarrow {}^4I_{11/2}$ (Nd^{3+}), $^4F_{3/2} \rightarrow {}^4I_{13/2}$ (Nd^{3+}), $^4I_{13/2} \rightarrow {}^4I_{15/2}$ (Er^{3+}), $^4I_{9/2} \rightarrow {}^4I_{13/2}$ (Er^{3+}), $^4I_{13/2} \rightarrow {}^4I_{9/2}$ (Nd^{3+}) in f-shells of both rare earth metals. The glass matrix's high transmittance values and intense photoluminescence caused by Er^{3+} and Nd^{3+} make them suitable for designing optoelectronic devices for working in the near and mid – IR ranges.

K e y w o r d s: chalcogenide glasses; Ga_2S_3–GeS_2–Sb_2S_3 system, rare earth metals, optical absorption, photoluminescence, IR materials.

1. Introduction

Sulfur-containing glasses are wide-gap semiconductors, which are characterized by high transparency in a wide range of wavelengths, high refractive index, low optical losses, and nonlinear optical properties [1–3]. In addition, they exhibit high thermal and mechanical strength, and radiation resistance and are a good environment for introducing rare earth (RE) metals. Due to such important properties, chalcogenide glasses are widely used as compact optical fibers, non-contact sensors, optical amplifiers, and photoelectrodes [4–8].

Sulfide glasses doped with RE metals are highly attractive as light-emitting media due to their optical

properties and low energy of phonons, which results in a reduced probability of non-radiative transitions and energy losses. Scientists are focusing on studying the photoluminescence (PL) properties of sulfides in the visible, near, and mid-IR regions, as the glasses are effective light-emitting media when doped with RE metals. Typically, they are doped with a single RE metal, with varying concentrations.

Among sulfide glasses, the most studied in terms of structure, optical, and luminescence properties are Ga_2S_3–GeS_2 glasses doped with RE. They are characterized by high transparency in a wide spectral range, which contributes to the high efficiency of RE radiation in the visible and near-IR ranges [9, 10]. The disadvantage of these glasses is their high tendency for crystallization and inhomogeneous distribution of RE in the glass-forming matrix, which can lead to concentration quenching of PL [11]. To reduce the impact of these negative factors, an additional component Sb_2S_3 is added to the matrix [12]. This leads to a decrease in the glass transition temperature T_g and crystallization temperature T_c, an increase in the refractive index, and a decrease in the band gap [6, 12]. Glasses of the Ga_2S_3–GeS_2–Sb_2S_3 quasi-ternary system doped with RE exhibit interesting PL properties, especially in the mid-infrared range [6, 13, 14].

The purpose of the work is to study the optical properties of 20 mol.% Ga_2S_3 – 60 mol.% GeS_2 – 20 mol.% Sb_2S_3 glasses double-doped with Er and Nd ions by varying their ratio. This significantly increases the possibility of controlling radiation spectra and helps predict the use of such systems as light-emitting media in optoelectronic technology.

2. Synthesis of the Glasses, Methodology, and Experimental Techniques

The synthesis of the glasses was carried out in quartz ampoules pumped out to a residual pressure of 0.1 Pa from high-purity elements: Ga – 99.999%, Ge – 99.999%, Sb, Nd, Er – 99.99% and S – 99.997% (sulfur was previously purified by double vacuum distillation). The concentration of Er in the glasses varied from 1 to 4 mol.% and the Nd concentration in all samples was 2 mol.%. The synthesis of the samples was carried out by the direct one-temperature method in mine-type furnace with accuracy of temperature control of ± 5 K. Batches in the first stage were heated at a rate of 10 K/h to 400 K (48 h of annealing), then to 720 K (48 h of annealing), and
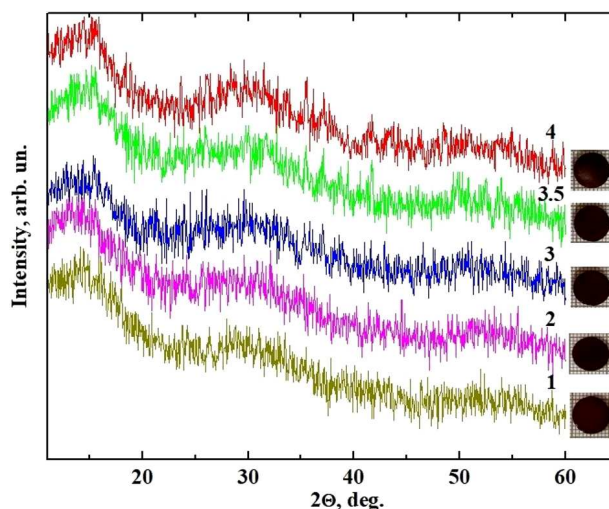

Fig. 1. X-ray diffraction patterns of the 20 mol.% Ga_2S_3 – 60 mol.% GeS_2 – 20 mol.% Sb_2S_3 : (1–4) mol.% Er; 2 mol.% Nd (Numbers indicate mol.% Er. To the right of the diffractograms are photos of the samples)

finally to a maximum temperature of 1210 K, (2 h of annealing), then cooled to room temperature at a speed of 20 K/h. The obtained alloys were crushed in an agate mortar, placed in quartz containers with a spherical bottom (diameter 1 cm), and pumped down to the residual pressure of 0.1 Pa. Then the samples were reheated at a rate of 50 K/h to 1210 K. After the 2-hour annealing at the maximum temperature, the samples were quenched in a saturated salt solution with crushed ice.

X-ray phase analysis of the synthesized samples proved that they are characterized by an amorphous state, and no crystalline inclusions were registered (Fig. 1). X-ray diffraction patterns of the samples were recorded on a DRON 4-13 diffractometer ($Cu K_\alpha$-radiation).

For the registration of the Raman spectra, the spectrometer MDR-23 equipped with a cooled CCD detector iDus 420 Andor (UK) was used. The Raman signals were excited by using the diode-pumped solid-state laser line at 532 nm. The laser power density on the sample surface was less than 10^3 W/cm^2, to preclude any thermal modification of the samples. A spectral resolution did not exceed 4 cm^{-1} and was determined from the Si phonon peak width of a Si single crystal. The Si phonon peak position of 520.5 cm^{-1} was used as a reference for determining the position of the peaks in the Raman spectra.
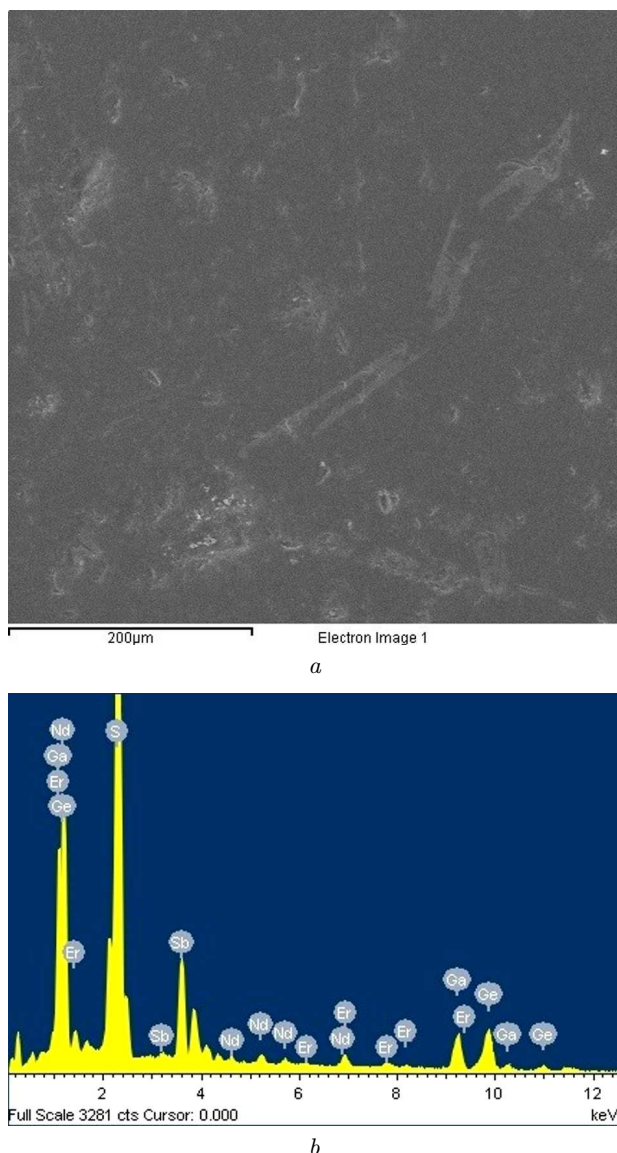
Fig. 2. SEM image of the surface microstructure of the glasses 20 mol.% Ga_2S_3 – 60 mol.% GeS_2 – 20 mol.% Sb_2S_3: 4 mol.% Er; 2 mol.% Nd (*a*); EDS spectrum of the glasses 20 mol.% Ga_2S_3 – 60 mol. % GeS_2 – 20 mol.% Sb_2S_3: 4 mol.% Er; 2 mol.% Nd, from which its composition was determined (*b*)

The morphology of the samples was studied using scanning electron microscopy (Tescan Mira 3 MLU) with an accelerating voltage of 520 kV. Energy-dispersive X-ray (EDX) spectra were taken using a built-in Oxford X-max 80 mm^2 setup.

Using scanning electron microscopy (SEM), an image of the surface of the glasses with 4% Er, 2%

Nd was obtained (Fig. 2, *a*). Energy dispersive X-ray spectroscopy (EDS) analysis confirmed the composition of the synthesized sample, which is in good agreement with the calculated composition. The quantitative amounts of elements are shown in Fig. 2, *b*.

Spectra of optical absorption and photoluminescence were obtained using MDR-204 monochromator. The signal was recorded by Si and PbS photosensors. The samples were prepared as parallel-plane plates of 1 mm in thickness. Emission of a diode laser with the wavelength at 805 nm was used for excitation of PL. Fourier spectrometer IRAffinity-1S was used for investigation transmission spectra in the range of 500–7500 cm^{-1}.

3. Results and Discussion

3.1. Visible and IR absorption spectra and Raman scattering of light

The optical absorption spectra of 20 mol.% Ga_2S_3 – 60 mol.% GeS_2 – 20 mol.% Sb_2S_3 glasses double-doped with Er and Nd were studied in the range of 550–2000 nm at room temperature (Fig. 3). The optical absorption edge of glasses exists at 600 nm and does not change significantly after adding Er and Nd. The samples demonstrate high transparency in the spectral range of 700–2000 nm. At the same time, narrow absorption bands with maxima at 655, 755, 810, 885, 980, and 1540 nm corresponding to the f-shell transitions of Er^{3+} and Nd^{3+} were registered. As the Er content increases, the intensities of the absorption bands associated with the impurity Er ions increase.

The transmission spectra of glasses with minimum (1 mol.%) and maximum Er content (4 mol.%) are shown in Fig. 4. The band with the absorption maximum at 6505 cm^{-1} (1540 nm) is associated with Er^{3+}; at 3950 cm^{-1} (2530 nm) is a band caused by overlapping transitions in the f-shells of Er^{3+} and Nd^{3+}; 1940 cm^{-1} (5150 nm) is associated only with Nd^{3+}. Additionally, a band with a maximum of 2500 cm^{-1} (4000 nm) was fixed, which corresponds to S–H bonds. The high value of the transmittance indicates the possibility of using the glasses of the Ga_2S_3–GeS_2–Sb_2S_3 system as optical elements in devices for the near and mid-IR ranges.

Samples with different amounts of erbium and neodymium were studied with Raman spectroscopy. The obtained spectra were similar, therefore, the Ra-
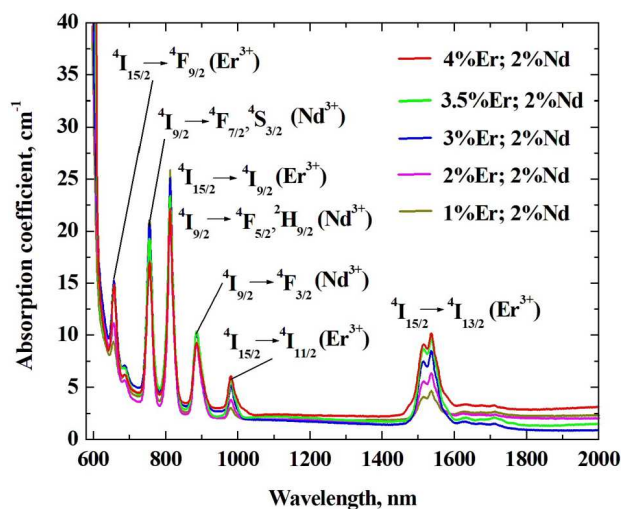
Fig. 3. The optical absorption spectra for the glasses 20 mol.% Ga_2S_3 – 60 mol.% GeS_2 – 20 mol.% Sb_2S_3: 1–4 mol.% Er; 2 mol.% Nd

Fig. 4. The transmission spectra for the glasses 2 mol.% Ga_2S_3 – 60 mol.% GeS_2 – 20 mol.% Sb_2S_3: 1, 4 mol.% Er; 2 mol.% Nd

man spectrum with the maximum erbium content is shown as a typical one (Fig. 5). It shows that the corresponding glasses without crystalline inclusions were formed during the synthesis process.

Figure 5 shows the experimental Raman spectrum of the $20Ga_2S_3$–$60GeS_2$–$20Sb_2S_3$: Er; Nd sample and its decomposition into individual components. Its decomposition was carried out tin view of the fact that the studied glass consists of a network of certain structural units of compounds Ga_2S_3, GeS_2, and Sb_2S_3. As known for GeS_2 and Ga_2S_3, the basic structural units in glass are $[GeS_{4/2}]$ ($[GaS_{4/2}]$) tetrahedra, which can be connected by a shared corner, a shared edge, or through a bridging sulfur atom [15], and trigonal pyramids $[SbS_3]$ [16].

Note that the most intense band in the Raman spectra of GeS_2 glass with a frequency of 343 cm^{-1} and symmetry $\nu_1(A_1)$ is attributed to the symmetric stretching vibrations of tetrahedra connected through a common corner [17]. This band in the spectra is always accompanied by its companion modes (A_1^c) [15] with a frequency of $\sim$370 cm^{-1}, which is a manifestation of symmetrical stretching vibrations of $[GeS_{4/2}]$ tetrahedra connected through a common edge. Less intense is the band of asymmetric stretching vibrations of tetrahedra connected through a common corner $\nu_3(F_2)$ with a frequency of $\sim$402 cm^{-1} [17, 18]. The frequency position of 438 cm^{-1} is characteristic of the companion modes (A_1^c) of $\nu_3(F_2)$ [18]. The
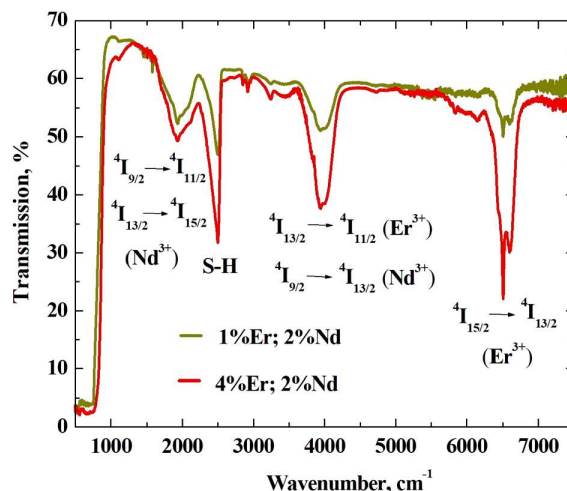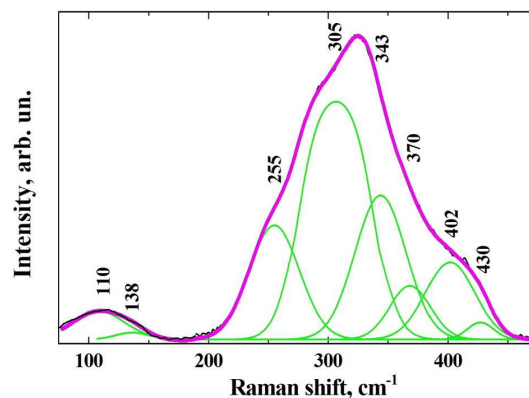

Fig. 5. The Raman spectrum of the sample 20 mol.% Ga_2S_3 – 60 mol.% GeS_2 – 20 mol.% Sb_2S_3: 4 mol.% Er; 2 mol.% Nd

frequency is approximately the same for structural units S_3Ge – S – GeS_3 [6]; so, it is not possible to separate them.

Bands with a frequency of 110 and 138 cm^{-1} correspond to symmetric and asymmetric bending vibrations of $\nu_2(E)$ and $\nu_4(F_2)$ modes in $[GeS_4]$ tetrahedral [17]. The band with a frequency of 255 cm^{-1} corresponds to Ge–Ge vibrations in ethyl-like S_3Ge–GeS_3 structural units [19]. The broad band with a frequency of $\sim$305 cm^{-1} corresponds to the superposition of the symmetric and asymmetric vibrational stretching mode of $[SbS_3]$ pyramids [20]. Note that, since the atomic masses of Ga and Ge are quite close, the vibration frequencies of the $[GaS_4]$ tetrahedra of the corresponding vibrational modes (ν_i)
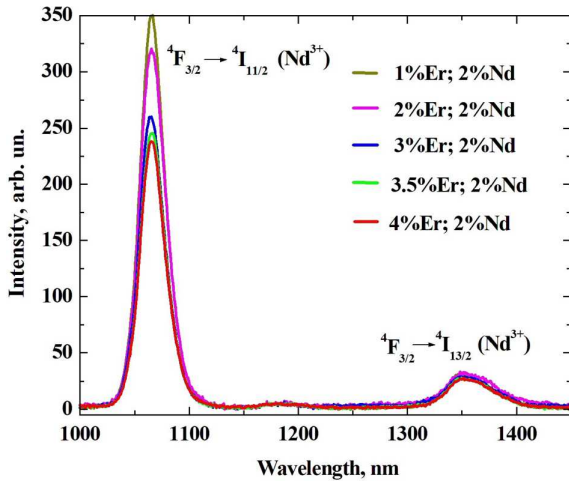
Fig. 6. The PL spectra of 20 mol.% Ga_2S_3 – 60 mol.% GeS_2 – 20 mol.% Sb_2S_3: 1–4 mol.% Er; 2 mol.% Nd glasses in the 1000–1450 nm region
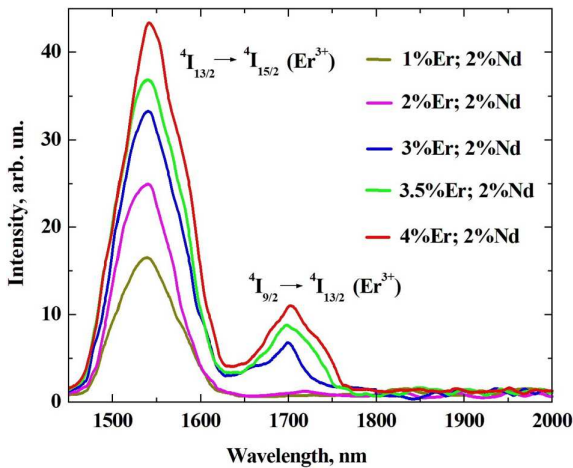

Fig. 7. The PL spectra of 20 mol.% Ga_2S_3 – 60 mol.% GeS_2 – 20 mol.% Sb_2S_3: 1–4 mol.% Er; 2 mol.% Nd glasses in the 1450–2000 nm region

practically coincide with the frequency of the corresponding vibrations of [GeS_4] tetrahedra. This leads to a broadening of the above-mentioned bands from [GeS_4] structural units.

3.2. Photoluminescent properties of glasses

As can be seen from Fig. 3, the absorption bands in the interval 790–820 nm correspond to the transitions $^4I_{15/2} \to {}^4I_{9/2}$ (Er^{3+}) and $^4I_{9/2} \to {}^4F_{5/2}$, $^2H_{9/2}$ (Nd^{3+}) in the *f*-shells of the RE ions. Therefore, exciting laser radiation with a wavelength of 805 nm was chosen to study the photoluminescent properties of
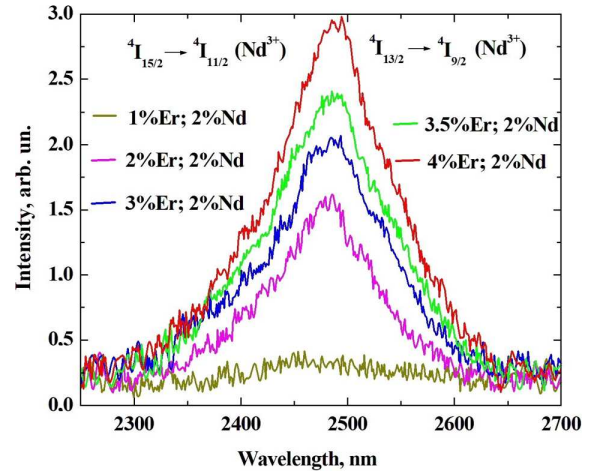

Fig. 8. The PL spectra of 20 mol.% Ga_2S_3 – 60 mol.% GeS_2 – 20 mol.% Sb_2S_3: 1–4 mol.% Er; 2 mol.% Nd glasses in the 2250–2700 nm region

the obtained glasses. This approach made it possible to analyze the emission efficiency of Er^{3+} and Nd^{3+} ions in a wide spectral range when they were simultaneously excited by radiation with the same wavelength. The obtained emission spectra of the glasses 20 mol% Ga_2S_3 – 60 mol.% GeS_2 – 20 mol.% Sb_2S_3 doped with 1–4 mol.% Er and 2 mol% Nd are presented in Figs. 6–8.

Five bands of the PL with maxima at 1070, 1350, 1540, 1700, and 2490 nm, corresponding to the transitions $^4F_{3/2} \to {}^4I_{11/2}$ (Nd^{3+}), $^4F_{3/2} \to {}^4I_{13/2}$ (Nd^{3+}), $^4I_{13/2} \to {}^4I_{15/2}$ (Er^{3+}), $^4I_{9/2} \to {}^4I_{13/2}$ (Er^{3+}), $^4I_{13/2} \to {}^4I_{9/2}$ (Nd^{3+}) in the f-shells of the ions were fixed. The appearance of many emission bands in the IR range of the spectrum prompts us to use the diagrams of energy levels in Er^{3+} and Nd^{3+} ions to explain the emergence of excited states and their relaxation mechanism (Fig. 9).

When light with a wavelength of 805 nm has been applied, Er^{3+} and Nd^{3+} ions become excited and move from their ground states to excited states of $^4I_{9/2}$ (Er^{3+}) and $^2H_{9/2}$, $^4F_{5/2}$ (Nd^{3+}). The PL, with a maximum of 1700 nm, is determined by the transition $^4I_{9/2} \to {}^4I_{13/2}$, and at 1540 nm is another transition $^4I_{13/2} \to {}^4I_{15/2}$ in Erbium ions. Nonradiative relaxation to the $^2H_{3/2}$, $^4F_{3/2}$ states in Nd^{3+} ions occurs due to the emergence of excited states $^2H_{9/2}$, $^4F_{5/2}$. This nonradiative transition occurs because the energy distance between these states is quite small (~ 1000 cm^{-1}) [21, 22]. As evidenced by Raman spec-
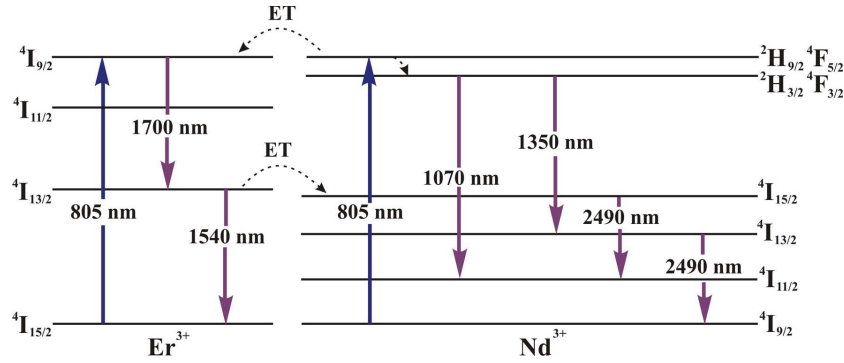
Fig. 9. Energy level diagram of Er^{3+} and Nd^{3+} ions

troscopy studies (Fig. 5), the maximum phonon energy of the glass matrix is $\sim$430 cm^{-1}, so the $^2H_{9/2}$ ($^4F_{5/2}$) $\rightarrow$ $^2H_{3/2}$ ($^4F_{3/2}$) transition can be accompanied by the excitation of 2 or 3 matrix phonons.

The formation of excited states $^2H_{3/2}$, $^4F_{3/2}$ leads to the appearance of PL bands at 1070 and 1350 nm (transitions $^4F_{3/2} \rightarrow {}^4I_{11/2}$ (Nd^{3+}), $^4F_{3/2} \rightarrow {}^4I_{13/2}$ (Nd^{3+}), respectively). In turn, the occurrence of excited states $^4I_{13/2}$ (Nd^{3+}) determines the transition $^4I_{13/2} \rightarrow {}^4I_{9/2}$ (Nd^{3+}) and, accordingly, PL emission (band – 2490 nm).

As can be seen from Fig. 6, an increase in the erbium content leads to a decrease of the most intense PL band at 1070 nm associated with Nd^{3+} ions. At the same time, the PL intensity with the maxima at 1540 and 1700 nm associated with Er^{3+} ions increases. They are associated with a competing radiation channel, namely with transitions in the f-shells of Er^{3+} ions. As can be seen from the diagram (Fig. 9), excited states $^2H_{9/2}$, and $^4F_{5/2}$ can further relax into states $^2H_{3/2}$, and $^4F_{3/2}$ or through energy transfer (ET) to transmit energy to Er^{3+} ions, since energy states $^4I_{9/2}$ (Er^{3+}) and $^2H_{9/2}$, $^4F_{5/2}$ (Nd^{3+}) are close. It is known [23] that the probability of ET depends on the concentration and distance between ions:

$$W_{ET} \propto \frac{1}{R^6} \propto n^2, \qquad (1)$$

where: R, n are the distance and concentration of ions between which ET is carried out.

At the same time, the probability of nonradiative multiphonon relaxation does not depend on the concentration of RE ions, while it depends on the electron-phonon interaction and increases exponentially with a decrease in the energy distance between the nearest states in the RE metals [24]:

$$W_{mph} = W_0 \cdot \{n(T) + 1\}^p \cdot e^{-\alpha \cdot \Delta E}, \qquad (2)$$

where: $\Delta E = p \cdot h\nu$ – the energy gap between the two nearest states of Nd^{3+} ions; p – the number of phonons; $h\nu$ – phonon energy; $n(T)$ – Bose–Einstein distribution; α, W_0 – are considered as empirical parameters that depend on the glass-forming matrix but are insensitive to rare-earth ions and energy states. In particular, for sulphide glasses $\alpha = 2.9 \times 10^{-3}$ cm, $W_0 = 10^6$ c^{-1} [25].

Therefore, an increase in the concentration of Er^{3+} leads to ET between Er^{3+} and Nd^{3+}, as a result of which the intensity of the PL bands with maxima at 1540 and 1700 nm increases. At the same time the intensity of the PL bands with maxima at 1070 and 1350 nm decreases, which we associate with the competing channel – multiphonon relaxation in Nd^{3+}. In addition, due to the energetic closeness of the $^4I_{13/2}$ (Er^{3+}), $^4I_{15/2}$ (Nd^{3+}) states and the ET process, the intensity of the band with a maximum at 2490 nm increases ($^4I_{15/2}$ (Nd^{3+}) $\rightarrow {}^4I_{11/2}$ (Nd^{3+}) transition). The influence of ET processes and nonradiative relaxation on PL intensity was noted in many works in the study of both chalcogenide glasses [26, 27, 28] and crystals [29, 30], as well as phosphate and borate [31, 32] glasses doped with RE metals.

Note that the authors [33] registered PL in $Ga_5Ge_{20}Sb_{10}S_{65}$ and $Ga_5Ge_{20}Sb_5S_{70}$ glasses doped with Nd^{3+} ions in the range of 2400–2800 nm with a maximum around 2550 nm, which corresponds to the transition $^4I_{13/2} \rightarrow {}^4I_{9/2}$ (Nd^{3+}). In the glasses we studied, the contribution to PL with a maximum of 2490 nm is given by the $^4I_{15/2} \rightarrow {}^4I_{11/2}$ (Nd^{3+}), transition, which is due to an energy transfer from Er^{3+}

ions, which are in the $^4I_{13/2}$ state (Fig. 8). Thus, the PL emission caused by the $^4I_{15/2} \rightarrow {}^4I_{11/2}$ transition contributes to the shift of the maximum of the PL band (which is a superposition of the abovementioned two transitions) to shorter wavelengths, and an increase in the erbium content leads to an increase in the PL intensity.

The low-energy band with a maximum of 2490 nm is extremely important in the applied aspect, e.g. in the construction of high-precision rangefinders based on light-emitting media, laser knives in medicine, and for monitoring the air pollution in environmental studies. Therefore, its enhancement when adding a coactivator (Er^{3+}) through the ET mechanism is an important factor for the creation of optoelectronic devices operating in the mid-infrared range.

4. Conclusions

Glasses of 20 mol.% Ga_2S_3 – 60 mol.% GeS_2 – 20 mol.% $Sb_2S_3 : Er_2S_3$ (1–4 mol.%); Nd_2S_3 (2 mol.%) composition were obtained by the quenching technique. Absorption bands with maxima at 655, 755, 810, 885, 980, and 1540 nm were recorded, which correspond to transitions in the f-shell of Er^{3+} and Nd^{3+} ions. Raman spectroscopy studies indicate that the main structural units of the glass matrix are $[Ge(Ga)S_4]$ tetrahedra and $[SbS_3]$ pyramids.

Under excitation by 805 nm laser radiation the PL bands with maxima at 1070, 1350, 1540, 1700, and 2490 nm were recorded in the near and mid-IR ranges (1000–2700 nm). Based on the diagrams of Er^{3+} and Nd^{3+} energy levels, the excited states in RE ions and the mechanism of radiation are explained. An increase in the Er content leads to a decrease in the intensity of the PL bands associated with Nd^{3+} and a simultaneous increase in the PL associated with Er^{3+}, because of the energy transfer between them.

High transmittance values (∼60–70%) and an intense PL band (maximum 2490 nm) create prerequisites for construction based on 20 mol.% Ga_2S_3 – 60 mol.% GeS_2 – 20 mol.% $Sb_2S_3 : Er_2S_3$ (1–4 mol.%); Nd_2S_3 (2 mol.%) glasses of active optical media for optoelectronic technology operating in the mid-IR range.

1. W. Blanc, Y.G. Choi, X. Zhang, M. Nalin *et al.* The past, present and future of photonic glasses: A review in homage to the United Nations International Year of glass 2022. *Prog. Mater. Sci.* **134**, 101084 (2023).

2. V.V. Halyan, V.O. Yukhymchuk, Ye.G. Gule, K. Ozga *et al.* Photoluminescence features and nonlinear-optical properties of the $Ag_{0.05}Ga_{0.05}Ge_{0.95}S_2$–$Er_2S_3$ glasses. *Opt. Mater.* **90**, 84 (2019).

3. A.M.El. Naggar, A.A. Albassam, G. Lakshminarayana, V.V. Halyan *et al.* Exploration of nonlinear optical features of Ga_2S_3–La_2S_3 glasses for optoelectronic applications, *Glass Phys. Chem.* **45**, 467 (2019).

4. T.V. Moreno, L.C. Malacarne, M.L. Baesso *et al.* Potentiometric sensors with chalcogenide glasses as sensitive membranes: A short review. *J. Non-Cryst. Solids.* **495**, 8 (2018).

5. V.V. Halyan, I.V. Kityk, A.H. Kevshyn, I.A. Ivashchenko *et al.* Effect of temperature on the structure and luminescence properties of $Ag_{0.05}Ga_{0.05}Ge_{0.95}S_2$–$Er_2S_3$ glasses. *J. Lumin.* **181**, 315 (2017).

6. A. Tverjanovich, Y.S. Tveryanovich, C. Shahbazova. Structure and luminescent properties of glasses in the GeS_2-Ga_2S_3-$Sb_2S_3 : Pr^{3+}$ system. *Materials* **16**, 4672 (2023).

7. M.M. Gul, K.S. Ahmad, A.G. Thomas, L. Almanqur *et al.* A clear path to enhanced performance: $In : SnO_2/(Er_2S_3$–ZrS_3–$NiS_2)GO$ as an effective transparent electrode in photoelectrochemical cells. *Mater. Chem. Phys.* **309**, 128445 (2023).

8. V.V. Halyan, A.H. Kevshyn, G.Ye. Davydyuk *et al.* IR Photoluminescence in $Ag_{0.05}Ga_{0.05}Ge_{0.95}S_2$–$Er_2S_3$. *Ukr. J. Phys.* **55**, 1278 (2010).

9. A.A. Man'shina, A.V. Kurochkin, S.V. Degtyarev, Ya.G. Grigor'ev *et al.* Glasses of the Ga_2S_3-GeS_2 system doped with rare-earth ions (Nd^{3+}, Er^{3+}) as active optical materials. In: *Proc. SPIE International Seminar on Novel Trends in Nonlinear Laser Spectroscopy and High-Precision Measurements in Optics* **4429**, 80 (2001).

10. Z.G. Ivanova, V.S. Vassilev, E. Cernoskova, Z. Cernosek. Physicochemical, structural and fluorescence properties of Er-doped Ge–S–Ga glasses. *J. Phys. Chem. Solids.* **64**, 107 (2003).

11. Y.S. Tver'yanovich. Concentration quenching of luminescence of rare-earth ions in chalcogenide glasses. *Glass Phys. Chem.* **29**, 166 (2003).

12. M. Ichikawa, T. Wakasugi, K. Kadono. Glass formation, physico-chemical properties, and structure of glasses based on Ga_2S_3–GeS_2–Sb_2S_3 system. *J. Non-Cryst. Solids.* **356**, 2235 (2010)

13. M. Ichikawa, Y. Ishikawa, T. Wakasugi, K. Kadono. Mid-infrared emissions from Ho^{3+} in Ga_2S_3–GeS_2–Sb_2S_3 glass. *J. Lumin.* **132**, 784 (2012).

14. M. Ichikawa, Y. Ishikawa, T. Wakasugi, K. Kadono. Near- and mid-infrared emissions from Dy^{3+} and Nd^{3+}-doped Ga_2S_3–GeS_2–Sb_2S_3 glass. *Opt. Mater.* **35**, 1914 (2013).

15. J. Heo, J.M. Yoon, S-Y. Ryou. Raman spectroscopic analysis on the solubility mechanism of La_3 in GeS_2–Ga_2S_3 glasses. *J. Non-Cryst. Solids.* **238**, 115 (1998).

16. L. Koudelka, M. Frumar, M. Pisarik. Raman spectra of Ge–Sb–S system glasses in the S-rich region. *J. Non-Cryst. Solids.* **41**, 171 (1980).

17. G. Lucovsky, F.L. Galeener, R.C. Keezer *et al.* Structural interpretation of the infrared and Raman spectra of glasses in the alloy system $Ge_{1-x}S_x$. *Phys. Rev. B.* **10(12)**, 5134 (1974).

18. C. Julien, S. Barnier, M. Massot, N. Chbani *et al.* Raman and infrared spectroscopic studies of Ge–Ga–Ag sulphide glasses. *Mater. Sci. Eng. B* **22**, 191 (1994).

19. X.F. Wang, S.X. Gu, J.G. Yu, X.J. Zhao, H.Z. Tao. Structural investigations of GeS_2–Ga_2S_3–CdS chalcogenide glasses using Raman spectroscopy. *Solid State Commun.* **130**, 459 (2004).

20. H. Takebe, T. Hirokawa, T. Ichiki, K. Morinaga. Thermal stability and structure of Ge–Sb–S glasses, *J. Ceram. Soc. Jpn.* **111**, 572 (2003).

21. J.H. Campbell, T.I. Suratwala. Nd-doped phosphate glasses for high-energy/high-peak-power lasers. *J. Non-Cryst. Solids.* **263–264**, 318 (2000).

22. J-F, Wyart, A, Meftah, A. Bachelier, J. Sinzelle *et al.* Energy levels of $4f^3$ in the Nd^{3+} free ion from emission spectra, *J. Phys. B: At. Mol. Opt. Phys.* **39**, L77 (2006).

23. D.L. Dexter. A theory of sensitized luminescence in solids. *J. Chem. Phys.* **21**, 836 (1953).

24. C.B. Layne, W.H. Lowdermilk, M.J. Weber. Multiphonon relaxation of rare-earth ions in oxide glasses. *Phys. Rev. B.* **16**, 10 (1977).

25. R. Reisfeld, C.K. Jørgensen. Excited state phenomena in vitreous materials. Handbook on the physics and chemistry of rare earths. **9**, 1 (1987).

26. L. Li, J. Bian, Q. Jiao, Z. Liu *et al.* GeS_2–In_2S_3–CsI chalcogenide glasses doped with rare earth ions for near- and Mid-IR luminescence. *Sci. Rep.* **6**, 37577 (2016).

27. I.V. Kityk, V.V. Halyan, V.O. Yukhymchuk, V.V. Strelchuk *et al.* NIR and visible luminescence features of erbium doped Ga_2S_3–La_2S_3. *J. Non-Cryst. Solids.* **498**, 380 (2018).

28. V.V. Halyan, V.O. Yukhymchuk, I.A. Ivashchenko, V.S. Kozak *et al.* Synthesis and downconversion photoluminescence of Erbium-doped chalcohalide glasses of AgCl(I)–Ga_2S_3–La_2S_3 systems. *Appl. Opt.* **60**, 5285 (2021).

29. J. Ganem, S.R. Bowman. Use of thulium-sensitized rare earth-doped low phonon energy crystalline hosts for IR sources, *Nanoscale Res. Lett.* **8** (1), 455 (2013).

30. V.V. Halyan, O.Y. Khyzhun, I.A. Ivashchenko, A.H. Kevshyn *et al.* Electronic structure and optical properties of $(Ga_{70}La_{30})_2S_{300}$ and $(Ga_{69.75}La_{29.75}Er_{0.5})_2S_{300}$ single crystals, novel light-converting materials. *Physica B Condens. Matter.* **544**, 10 (2018).

31. M. Kuwik, C.K. Jayasankar, W.A. Pisarski, J. Pisarska. Theoretical calculations and experimental investigations of lead phosphate glasses singly doped with Pr^{3+} and Tm^{3+} ions using luminescence spectroscopy. *J. All. Comp.* **842**, 155801 (2020).

32. Ullah, F. Zaman, G. Rooh, S.A. Khattak *et al.* Photoluminescence and energy transfer investigations in Gd^{3+}-Dy^{3+} co-doped borate glasses. *Physica B: Condens. Matter.* **639**, 413976 (2022).

33. R. Chahal, F. Starecki, J-L. Doualan, P. Němec *et al.* Nd^{3+}:Ga–Ge–Sb–S glasses and fibers for luminescence in mid-IR: Synthesis, structural characterization and rare earth spectroscopy. *Opt. Mater. Express* **8**, 1650 (2018).

В.В. Галян, А.Г. Кевшин,
І.А. Іващенко, Т.К. Яцинюк, Б.А. Татарин,
М.А. Скорик, О.О. Лебедь, В.О. Юхимчук

ВИПРОМІНЮВАННЯ У БЛИЖНЬОМУ ТА СЕРЕДНЬОМУ ІНФРАЧЕРВОНОМУ ДІАПАЗОНІ СТЕКОЛ Ga₂S₃–GeS₂–Sb₂S₃: Er, Nd

Стекла 20 моль% Ga_2S_3 – 60 моль% GeS_2 – 20 моль% Sb_2S_3: Er_2S_3 (1–4 моль%); Nd_2S_3 (2 моль%) отримано методом гартування. На основі досліджень спектрів оптичного поглинання встановлено смуги поглинання із максимумами 655, 755, 810, 885, 980 і 1540 нм. При збудженні фотолюмінесценції випромінюванням з $\lambda = 805$ нм у спектрі з'являються смуги з максимумами при 1070, 1350, 1540, 1700 і 2490 нм, що відповідає переходам $^4F_{3/2} \rightarrow {}^4I_{11/2}$ (Nd^{3+}), $^4F_{3/2} \rightarrow {}^4I_{13/2}$ (Nd^{3+}), $^4I_{13/2} \rightarrow {}^4I_{15/2}$ (Er^{3+}), $^4I_{9/2} \rightarrow {}^4I_{13/2}$ (Er^{3+}), $^4I_{13/2} \rightarrow {}^4I_{9/2}$ (Nd^{3+}) у f-оболонках обох рідкоземельних металів. Високі значення коефіцієнта пропускання скляної матриці та інтенсивна фотолюмінесценція, зумовлена Er^{3+} та Nd^{3+}, роблять її придатною для розробки оптоелектронних пристроїв, які працюють в ближньому та середньому ІЧ-діапазонах.

К л ю ч о в і с л о в а: халькогенідні стекла, система Ga_2S_3–GeS_2–Sb_2S_3, рідкісноземельні метали, оптичне поглинання, фотолюмінесценція, ІЧ матеріали.